An analytical force and surface roughness model for cylindrical grinding of brittle materials

Ali Zahedi* and Bahman Azarhoushang

Institute for Precision Machining (KSF),
Furtwangen University of Applied Sciences,
Jakob-Kienzle-Strasse 17,
D-78054 Villingen-Schwenningen, Germany
Email: ali.zahedi@hs-furtwangen.de
Email: aza@hs-furtwangen.de
*Corresponding author

Abstract: In this paper, an analytical approach is proposed for the modelling of ground surface and grinding forces in cylindrical grinding of ceramic materials. The model incorporates the near-actual distribution of cutting grains over the grinding wheel surface and a kinematic approach for the engagement of the grains with the workpiece surface per grinding parameters and conditions. To interpret the stochastic engagement of arbitrary grains with the workpiece, and to distinguish the dominant material removal mechanism, fracture mechanics of single-grain indentation is applied. The approach based on the fracture mechanics accounts for grain size and geometry and material properties. The results of a previously performed research on single-grain scratch tests are taken for interpreting force and workpiece surface characteristics. Without losing generality, the model was applied to a cylindrical plunge grinding of an alumina ceramic. The experiments show qualitative agreement of model predictions with the experimental force and ground workpiece topography.

Keywords: cylindrical grinding; brittle ceramics; alumina; kinematic modelling; indentation mechanics; surface roughness; grinding force; ductile grinding.

Reference to this paper should be made as follows: Zahedi, A. and Azarhoushang, B. (2017) 'An analytical force and surface roughness model for cylindrical grinding of brittle materials', *Int. J. Abrasive Technology*, Vol. 8, No. 1, pp.68–81.

Biographical notes: Ali Zahedi obtained his Bachelor's in Fluid Mechanics and Heat Transfer from the Shiraz University in 2006 and Master's and PhD in Applied Mechanics from the Sharif University of Technology in 2009 and 2015 respectively. He is working in the Institute for Precision Machining (KSF), at the Furtwangen University of Applied Sciences, Germany as a Research Associate and Team Leader.

Bahman Azarhoushang graduated from the Sharif University of Technology, Iran, in 2006. He received his PhD in Mechanical Engineering from the Stuttgart University, Germany, in 2011. He was the Head of the Research and Development Department of Baerhausen Company before joining the Furtwangen University in 2013. Since September 2013, he is a member of Mechanical and Biomedical Engineering Faculty of Furtwangen University and simultaneously the Director of the Institute of Grinding and Precision Technology (KSF). He has published more than 50 papers in different languages. He has numerous lectures at national and international conferences

as proof of his research activities. He is an editor of the *Journal of Mechanical Sciences (MS)* and works as a reviewer of international journals *Machine Tools and Manufacture* (Elsevier) and *Advanced Manufacturing Technology* (Springer). Currently he works on various German national, DFG, AIF and BMFT projects.

This paper is a revised and expanded version of a paper entitled 'An analytical force and surface roughness model for cylindrical grinding of brittle materials' presented at The 20th International Symposium on Advances in Abrasive Technology ISAAT 2017. Okinawa, Japan, 3–6 December 2017.

1 Introduction

Advanced engineering ceramics gain ever-increasing attention especially for applications requiring high strength-to-weight ratio, stiffness, wears resistance, chemical and thermal stability. The manufacturing of high precision ceramic parts relies mostly on their grinding process, and accordingly, the economic feasibility of advanced ceramics is limited by their grinding efficiency (Malkin and Hwang, 2006). Comprehensive description of the material removal mechanisms of ceramics the prerequisite of the process optimisation and final product quality. Many researches have been aimed to provide this description, however, the exact mechanisms of ceramics grinding are not completely understood (Kitajima et al., 1992; Li et al., 2017). Extension of small-scale static indentation mechanics to the action of single grains on the workpiece surface was performed by some researchers, especially for brittle materials (Malkin and Hwang, 2006). Accordingly, two different regimes were distinguished for ceramics grinding: ductile regime and brittle regime. The dominant mechanisms during ductile and brittle grinding regimes are material pile-up and axial-lateral crack systems, respectively. It was suggested that the ductile regime governs until a critical grain depth-of-cut and, accordingly, a critical single-grain force values are reached (Bifano et al., 1991). However, the real dynamic conditions in grinding deviate from the static indentation analysis owing to the material properties at extremely large rates of deformation, irregular shape of the cutting grains and existence of a tangential force component. Modifications of the indentation analysis (Conway and Kirchner, 1980; Zahedi, 2015) and single-grain scratch tests and simulations (Tawakoli et al., 2013; Zahedi and Azarhoushang, 2016) are among the performed studies for investigating the material removal mechanisms of individual abrasive grains in grinding. The total material removal in grinding results from the rubbing and cutting actions in grain level. However, the random shape, orientation and the probabilistic distribution of the grains over the wheel body are further complications in the analysis of grinding process based on the action of individual grains. The distribution and shape of the cutting grains have been modelled based on different simplifying approaches. Among the various form assumptions, it was shown reasonable to consider the grain as spheres or cones with spherical tips for ceramics grinding (Agarwal and Rao, 2005; Agarwal and Venkateswara Rao, 2013; Shaw, 1972). Most researchers have considered uniform distribution of the cutting grain over the grinding wheel surface (Chen and Rowe, 1996; Stępień, 2007). Random and stochastic distribution of the cutting grains has been also considered in literature (Chang

and Junz Wang, 2008; Agarwal and Venkateswara Rao, 2010; Pinto et al., 2008). Considering different types and specifications of grinding wheels and the effects of conditioning conditions on the topography of the wheel surface, a comprehensive model should incorporate the near-actual and preferably measurement-based characteristics of the grinding wheel surface topography. In this aspect, a generalised model which could consider the kinematics of the grinding process along with its stochastic nature and the dominant material removal mechanisms for ceramics is not addressed in the present state of the art.

In this study, an analytical method is proposed for generating a dynamic relationship between the input and output parameters in cylindrical grinding of ceramic materials with respect to the actual stochastic grain distribution. The ductile material removal or brittle removal owing to crack generation and propagation, i.e., radial (median) and lateral crack systems are investigated. The grains are treated as cones of spherical tip with diameter corresponding to the average grain size of the grains. The inputs of the model include grinding wheel specifications and measured surface topography, kinematic grinding parameters, mechanical properties of the workpiece material, while the outputs encompass grinding force components, and topography of the ground ceramic workpiece. Integration of the kinematic model with the single-grain indentation model leads to a transient description of the cutting action performed by numerous abrasive grains on the wheel surface. As a case study, cylindrical plunge grinding of alumina round bars are conducted to verify the proposed model.

2 Mechanisms of ceramics grinding

Ductile grinding is the dominant mechanism in grinding of ceramics if the uncut chip thickness or grain penetration depth a_g does not exceed the critical value h_c defined as (Neo et al., 2012):

$$h_c = \Psi\left(\frac{E}{H}\right)\left(\frac{K_c}{H}\right)^2 \tag{1}$$

In the above equation E, H and K_c are the elasticity modulus, hardness and fracture toughness of the ceramic workpiece, respectively, while the material constant Ψ can be set equal to 0.15 for ceramic material in static and dynamic loading conditions (Sun et al., 2011). When a grain penetrates deeper in the workpiece surface ($a_g > h_c$), brittle cutting occurs through introduction of radial (median) and lateral cracks. As the cracks initiate at the edge of the plastic deformation zone, not only the critical uncut chip thickness value, but also the depth of plastic deformation zone a_p are of significance. Figure 1 illustrates the cutting mechanisms in ductile and brittle cutting regimes and corresponding surface phenomena under the action of normal force P in plastic (P_p) and crack initiation/propagation (P_c) limits. For a given grain diameter d_g with an indentation radius of a_i and groove cross-section of A_c, the pile-up can be assumed as triangles with height of h_p and contact angle of β.The ratio of the pile-up cross-section A_p to the groove cross-section A_c depends on the material properties and cutting conditions and will be addressed later. Knowing the cross-section ratio, it is possible to calculate the pile-up height and angle geometrically (Zahedi, 2015). Radial cracks penetrate into the workpiece surface and cause its strength reduction, while the lateral cracks contribute to

the material removal (Malkin and Hwang, 2006). The generation of the ground workpiece topography, therefore, requires the quantitative description of radial crack length C_R and lateral crack length C_l. The depth of the plastic deformation zone, where the two individual crack systems initiate, can be calculated according to the indentation mechanism corresponding to the critical grain depth of penetration ($a_g = h_c$). Therefore, the following expression was established for a spherical indenter of given dimensions on a ceramic workpiece (Zahedi, 2015):

$$a_p = (\pi/2)^{1/3} d_g \left(\frac{a_i}{d_g}\right)^{4/3} \left(\frac{E}{H}\right)^{1/2} \tag{2}$$

For a wide range of brittle materials and applied indentation forces, it has been shown (Van Der Zwaag et al., 1980; Chiang, 1982), that the measured hardness is independent of the indenter geometry. Therefore, the indentation radius in equation (2) could be expressed in terms of normal applied force and the hardness value as (Lawn and Swain, 1975):

$$a_i = \sqrt{P/\pi H} \tag{3}$$

Therefore, for given properties of the ceramic material and grain size, the depth of plastic deformation zone prior to crack initiation can be calculated.

The maximum radial crack length can be obtained according to the stress intensity factor around a median crack (Conway and Kirchner, 1980), but is of minor importance in the generation of the ground surface. Therefore, only the lateral cracks will be considered in the present modelling. The minimum force required for the generation of lateral cracks is (Chiang, 1982):

$$P_{cl}^{*} = \zeta \left(K_c{}^4 / H^3\right) f(E/H) \tag{4}$$

where ζ is a dimensionless constant and its product with the weak function $f(E / H)$ is approximately equal to 2×10^5 for ceramic materials (Malkin and Hwang, 1996). For an applied normal force P_c, the lateral crack length C_L can be expressed in terms of the critical normal force p_{cl}^{*} and a function c^l as shown in (Marshall et al., 1982).

$$C_L = c^l \left[1 - \left(P^{*}{}_{cl} / P_c\right)^{1/4}\right]^{1/2} \tag{5}$$

The expression presented in (Marshall et al., 1982) for c^l in case of a conical Vicker's indenter can be rearranged for a spherical grain as (Zahedi, 2015):

$$c^l = \left\{\left(2\zeta_L \sqrt{3}/3\right)\left(3\pi a_i / d_g\right)^{5/6} \left[\left(K_c H\right)^{-1} E^{3/4}\right]\right\}^{1/2} P_c^{5/8} \tag{6}$$

The dimensionless parameter ζ_l is independent of the indenter geometry and for a wide range of ceramics is equal to 25×10^{-3}. Equation (2), equation (3) and equation (5) define how the brittle grinding mechanism affects the workpiece surface by expressing the crack geometry and initiation in terms of material properties and applied normal force. However, they provide no information about the grain force and pile-up geometry, which are highly dependent on the dynamic characteristics and conditions of grinding process. Single-grain scratch test is a promising approach to resemble reliable information about

the material behaviour under actual dynamic grinding conditions. Therefore, to define the pile-up characteristics and the grain force components, the results of a previous work on the single-grain cutting of the same alumina ceramic are used in the present research. According to the single-grain scratch tests performed in Zahedi (2015), the normal grain force and the surface pile-up were measured for different cutting speeds and grain depths of cut. The surface pile-up was characterised by defining the pile-up ratio as the ratio of the pile-up to the groove cross-sections ($\eta_p = A_p / A_c$). Figure 2 presents a measured cross-section with corresponding pile-up and cut surface areas.

Figure 1 Grain-workpiece contact mechanisms under different load ranges in the plane normal to the cutting direction (a) plastic deformation (b) crack initiation and propagation (see online version for colours)

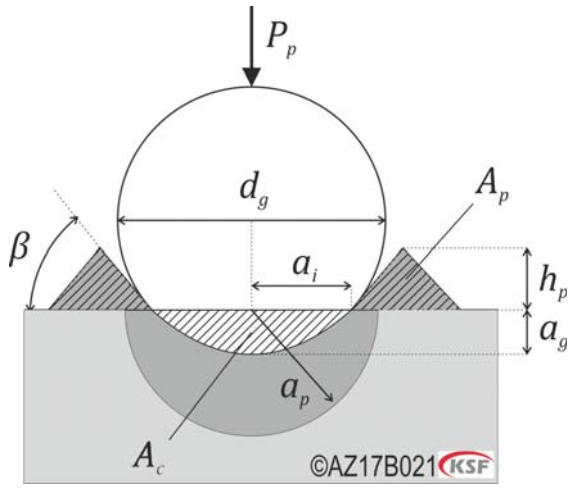

(a)

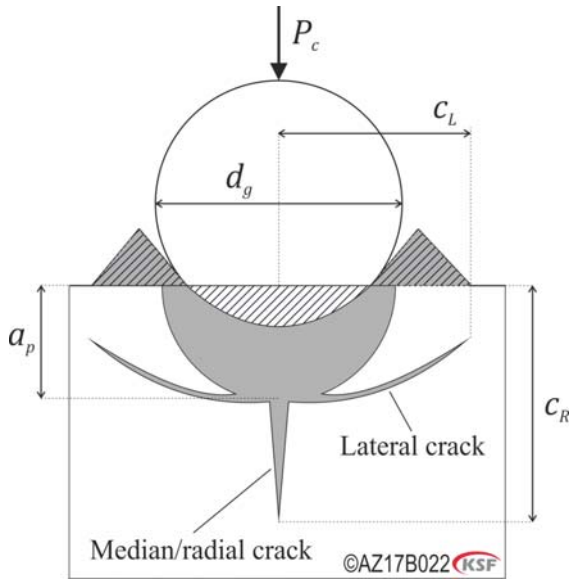

(b)

Figure 2 Measured cross-section of a scratch generated on alumina workpiece with cutting speed of 30 m/s (see online version for colours)

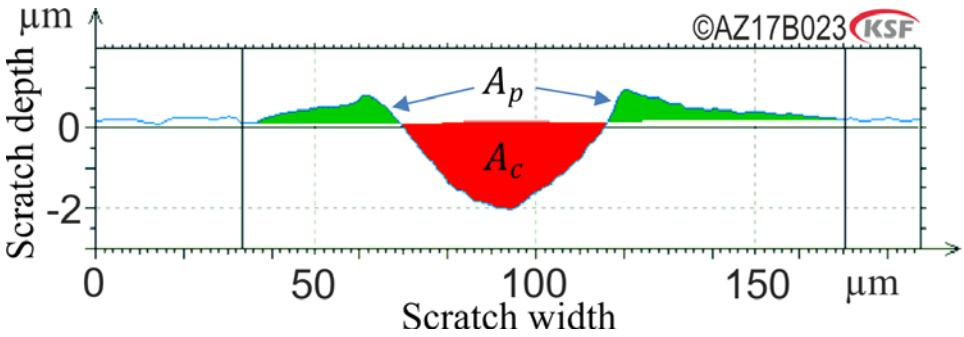

The discrete force and pile-up ratio data were extended to continuous functions of the process parameters by performing a data regression on the single-grain scratch tests. Accordingly, two functional forms were assumed for the grain force and pile-up ratio, which included unknown coefficients and exponents. The regression method was based on minimising the error of the assumed forms with respect to the experimental single-grain scratch test results by applying least square criteria. The assigned unknown factors could be calculated, and therefore, the following expressions were obtained for the normal grain force P and the pile-up ratio (Zahedi, 2015):

$$P = 0.125 d_g a_g^{0.6436} v_c^{-0.4725} \tag{7}$$

$$\eta_p = 1 - \left(6.969 \times 10^{-6} A_c^{1.2396} v_c^{0.5090}\right) \tag{8}$$

Equation (7) (d_g and a_g expressed in µm, and v_c in meters per second) implies that the grain force is directly proportional to the grain size and depth of cut, but inversely proportional to the cutting speed. The reduction of grain force with cutting speed can be associated with local heat accumulation at the grain tip and thermal softening of the material. According to equation (8) (A_c expressed in µm^2), larger cutting force and groove cross-section lead to more efficient chip formation in the ductile grinding regime (less pile-up). The grain-workpiece interaction discussed in this section will be extended to the multitude of grains in the following section.

3 Stochastic grinding wheel surface topography

The specification of the grinding wheel provided by the manufacturer delivers the information about the mass and volumetric portion of the grains in the bonding matrix. However, the exact height distribution, which has a characteristic effect on the grinding performance, depends not only on the wheel specifications, but also on the wheel conditioning, chip loading and wear of the grains. Therefore, in this study the actual condition of the grinding wheel prior to the grinding experiments is extracted by generating the histogram curve of the wheel surface from confocal microscopy. Figure 3 shows the confocal image, the histogram diagram and the Abbott-curve of the metal-bonded diamond grinding wheel (D151-C118 from Tesch) utilised throughout the

experiments. The average grain size and concentration of the wheel are 151 µm and 118, respectively.

The vertical axis in Figure 3 defines the range of height measurement. The upper and lower horizontal axes in Figure 3(b) correspond to the Abbott-curve and the histogram diagram of the measured topography points, respectively. The histogram diagram defines the percentage of the points on the topography of the sampled area which are located at a specific depth measured from the highest point of the surface (vertical axis). The Abbott curve is on the other hand the integral of the histogram values from the highest to the lowest point on the surface. Both quantities are representative of height distribution of the topography points, and therefore, could be used to model the actual grinding wheel surface with a simplified grain distribution as discussed in Zahedi (2016).

Figure 3 (a) Confocal surface topography (b) The histogram diagram combined with the Abbott-curve of the grinding wheel (see online version for colours)

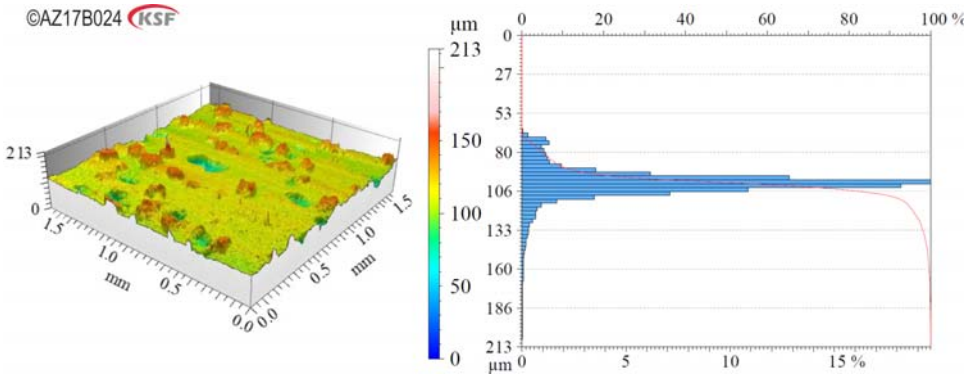

(a) (b)

The height distribution of the grains is modelled by establishing an analogy between the histogram diagram of the wheel topography and the shape and weight factors of a Gaussian distribution [according to the method presented in Zahedi and Azarhoushang, (2016)]. A view of the modelled wheel surface is illustrated in Figure 4.

The three-dimensional positions of the grains in the generated model are transferred to the kinematic analysis of the cylindrical grinding, where the engagement of individual grains with the workpiece can be detected. The details of the approach are presented in Zahedi and Azarhoushang (2016) and Zahedi et al. (2015). The criteria of engagement include the instantaneous calculation of the distance between grain centres (X_i, Y_i, Z_i) and the points assigned to the workpiece surface (X_j, Y_j, Z_j). Therefore, an engagement of the i^{th} grain occurs, whenever and as long as the following equation holds:

$$\left(X_i - X_j\right)^2 + \left(Y_i - Y_j\right)^2 + \left(Z_i - Z_j\right)^2 < \left(\frac{d_{g,i}}{2}\right)^2 \tag{9}$$

The grain-workpiece engagement can be interpreted according to the single-grain scratch mechanism, where the grain force and workpiece surface modification (pile-up in ductile regime or lateral crack propagation) are calculated according to the equivalent grain depth of cut a_g and the groove cross-section A_c in equation (7) and equation (8). This procedure will be repeated for all the grains on the grinding wheel surface for each time

step, where the force components are accumulated and the workpiece surface is modified by the grain action. As the workpiece surface is modified successively within the action of individual grains, the final workpiece surface topography includes the effects of whole grains, which come into contact with the workpiece.

Figure 4 Probabilistic model of the grain distribution over the grinding wheel surface (see online version for colours)

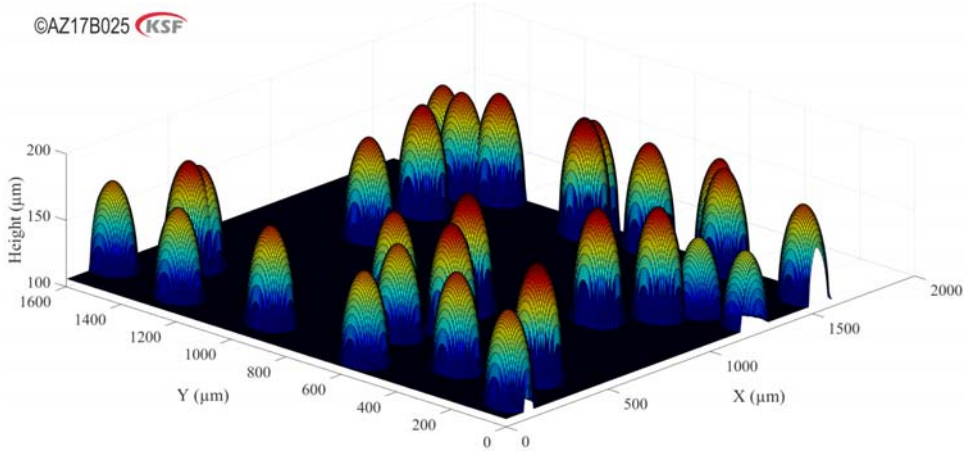

4 Grinding experiments

Cylindrical plunge grinding of alumina round bars with diameter of 20 mm was conducted on an EMAG SN204 CNC grinder with oil as grinding fluid. Grinding conditions are presented in Table 1 and a view of the experimental setup is shown in Figure 5. The grinding forces are measured using a rotary dynamometer (KISTLER 9124B) and the surface roughness is extracted using a Wavesystem Hommel tester T8000.

Table 1 Cylindrical grinding parameters

Cutting velocity [m/s]	10; 20; 30; 40
Infeed velocity [mm/min]	0.3; 0.6; 0.9; 1.2
Workpiece rotation speed [rpm]	300

The experimental (average values of three measurements) and modelled normal grinding forces are compared in Figure 6. The modelled force predictions exhibit the same trend as the experimental results, however, their absolute values are larger in all cases, especially in low cutting speeds. The minimum value of the average chip thickness within the selected set of grinding parameters and conditions occurs with the cutting velocity of 40 m/s and the infeed velocity of 0.3 mm/min. This minimum value could be approximated to be about 2.7 µm according to Chiang (1982) and is larger than the investigated (Zahedi, 2015) value of about 0.7 µm for the critical ductile-to-brittle chip thickness. In other words, the material removal takes place mainly in the brittle regime. However, the model is more precise for smaller chip thickness values in the lower range of the brittle

material removal mechanism. For lower cutting speeds, and correspondingly, average chip thickness values which could be larger than 7 µm for the cutting and infeed velocities of 10 m/s and 1.2 mm/min, respectively, the model is less accurate. The larger deviation of the simulated forces from the experimental measurements could be due to the underlying single-grain scratch test results, which were performed at grain cutting depths of up to 4 µm in (Zahedi, 2015). Performing single-grain scratch tests over a wider range of grain cutting depths, and accordingly, applying more accurate grain force expressions could improve the accuracy of the proposed model for a larger set of grinding parameters and conditions. Furthermore, the single-grain scratch tests are performed in dry conditions without applying coolant/lubricant, and therefore, could lead to larger forces in the model predictions. Assuming spherical form for the grains could also overestimate the grain forces as the actual sharp edges of the grains are missing, which could perform the material removal with smaller average forces.

Figure 5 Cylindrical grinding experimental setup (see online version for colours)

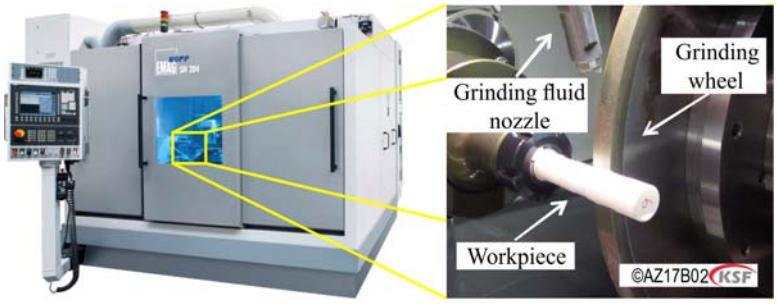

Figure 6 Comparison of modelled and measured normal grinding forces (see online version for colours)

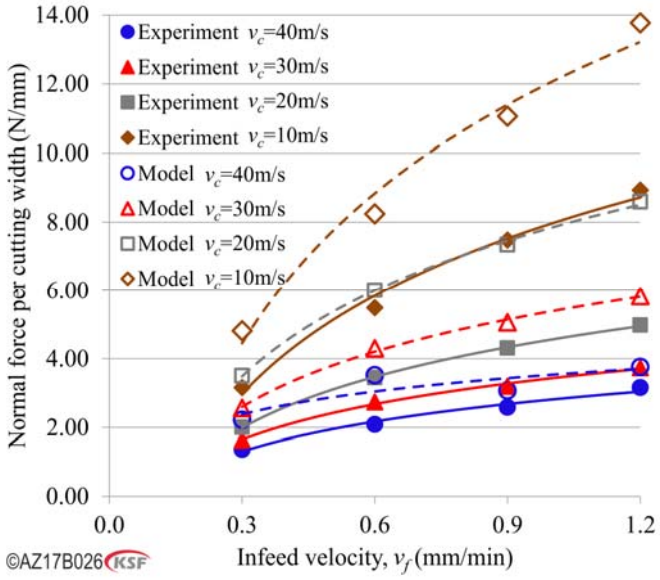

Figure 7 The modelled surface topography of the ground cylindrical workpiece (v_c = 40 m/s, v_f = 0.9 mm/min) (see online version for colours)

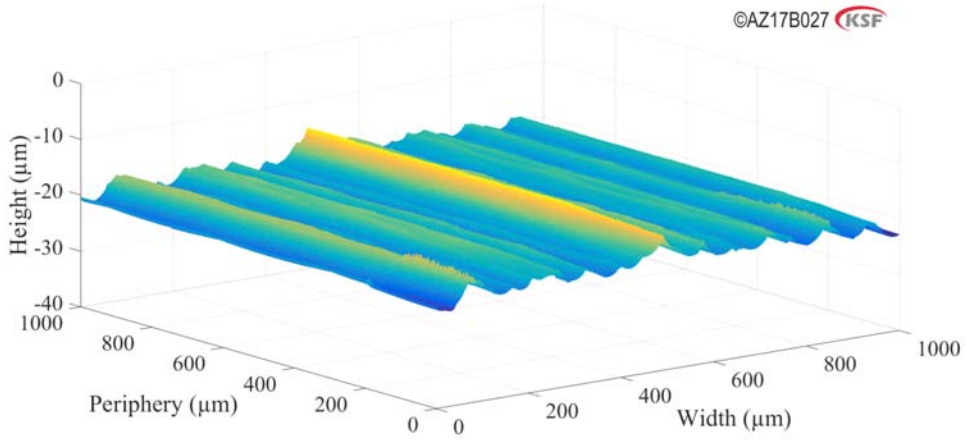

Figure 8 Measured topography of the ground workpiece surface across the grinding direction (v_c = 40 m/s, v_f = 0.9 mm/min) (see online version for colours)

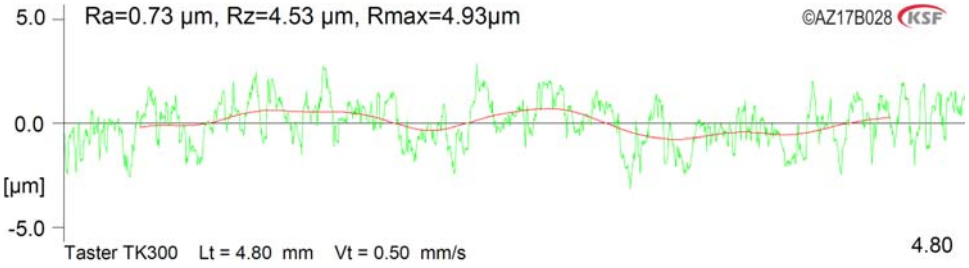

Figure 9 Topography of the modelled workpiece surface across the grinding direction (v_c = 40 m/s, v_f = 0.9 mm/min) (see online version for colours)

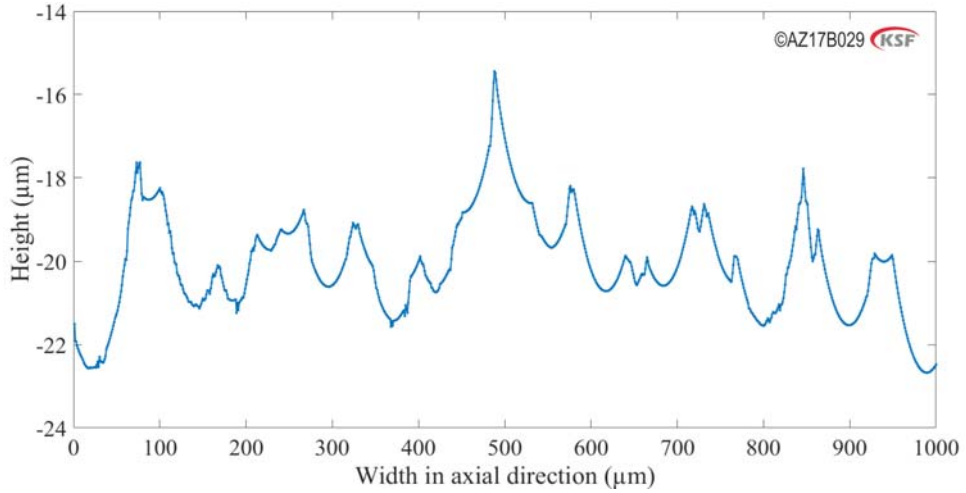

Figure 7 presents the modelled ground workpiece surface for the cutting velocity of 40 m/s, infeed velocity of 0.9 mm/min and workpiece rotation speed of 300 rpm. Correspondingly, Figure 8 and Figure 9 illustrate cross-sections measured on the actual ground workpiece surface and extracted from the modelled ground surface across the grinding direction, respectively. Figure 10 and Figure 11 show respectively that the measured average roughness R_a and maximum roughness R_{max} values are smaller than the model predictions on cross-sections equivalent to the one presented in Figure 9. This deviation in roughness values could be due to the inevitable spark-out phase, which occurs in cylindrical grinding in a short time after the end of grinding cycle and before the grinding wheel disengages from the workpiece zone. As a result, the wheel slightly smoothens the workpiece surface without infeed, and therefore, with ever-decreasing actual depth of cut. Assuming pure spherical grains could be also a source of deviation, as actual cutting grains are normally composed of sharp edges accompanied by flat areas, which could lead to finer surfaces. Furthermore, actual abrasive grains are subject to a degree of wear during the sharpening/dressing and grinding processes and some of them could be even broken or pulled out of the bond. Worn grains lead normally to smoother ground surface, which could also be associated with smaller measured roughness values in comparison with values of the modelled surface. Disregarding the broken or pulled-out grains and extending a theoretical grain distribution to the whole wheel surface in the proposed model could be another reason why the modelled force values are larger than the measured experimental ones.

Figure 10 Average roughness R_a of the measured (solid bars) and modelled (hatched bars) topography of the ground workpieces across the grinding direction (see online version for colours)

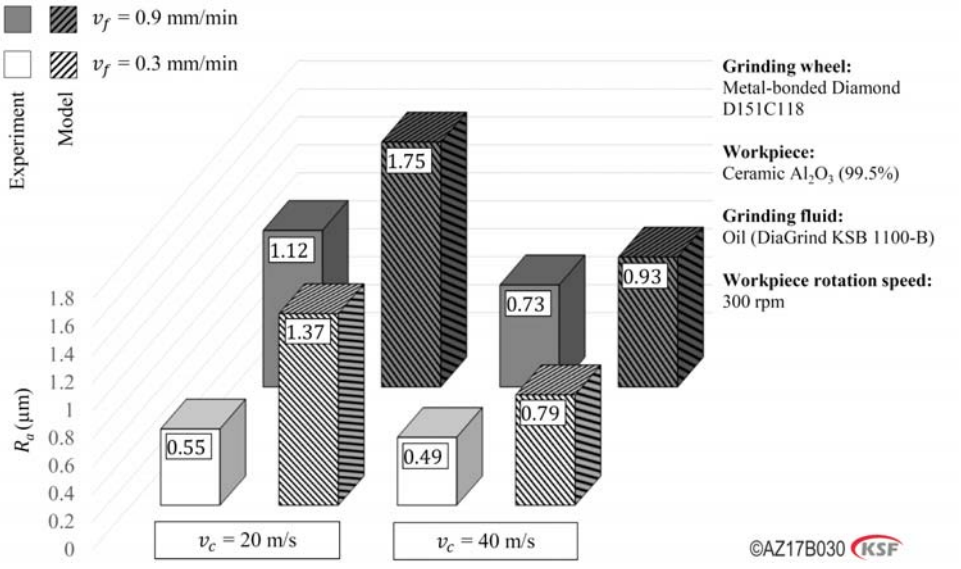

Figure 11 Maximum roughness R_{max} of the measured (solid bars) and modelled (hatched bars) topography of the ground workpieces across the grinding direction (see online version for colours)

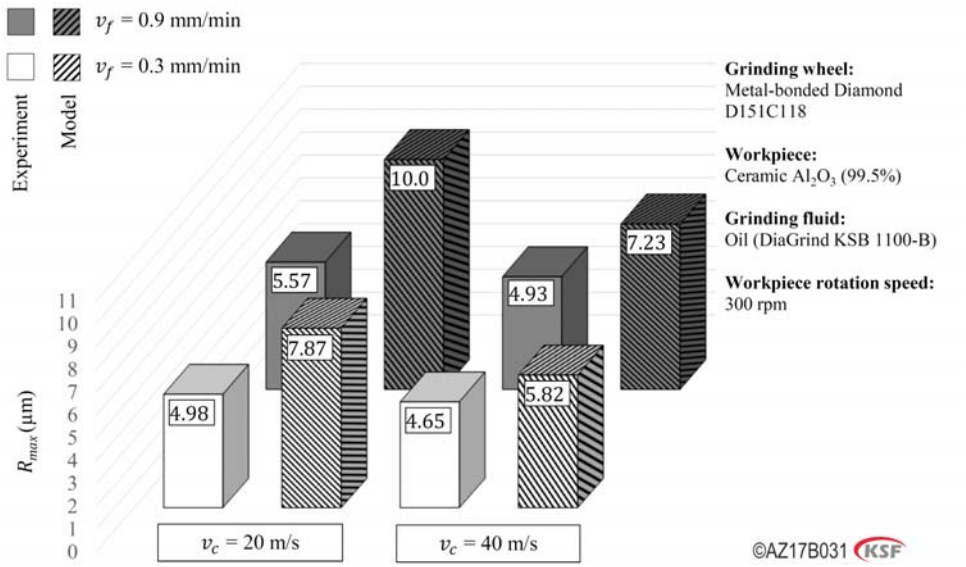

The force and ground surface topography model seems to provide acceptable results, which qualitatively agree with the cylindrical grinding experiments, however further improvements could be applied by assuming near-actual grain geometries, rubbing effects in the contact zone and lubrication conditions.

5 Conclusions

A generalised method was proposed to combine different material removal mechanisms of ceramics, stochastic grain distribution (based on topography measurement and flexible to the wheel conditioning) and kinematics of ceramics grinding, and to predict the grinding forces and ground workpiece topography. The model includes simplifying assumptions from the grain geometry (pure spherical) and distribution, to the material properties and cutting conditions. The grain height distribution was characterised by measuring the topography of actual wheel surface and correlating its histogram diagram above the mean height level (average height of bond surface) to the grain protrusion height. The predicted force and surface roughness values in the model follow the same qualitative trend as the experimental measurements. However, the modelled forces and roughness values are larger than the experimental results, which could be due to the simplified form of the grains, disregarding the actual spark-out at the end of experimental cycles, and the utilised single-grain scratch data. Considering more general grain geometries, the rubbing effects and elastic deformations in the contact zone, and the cooling-lubricating effects could improve the model accuracy. Furthermore, considering the grain wear and pull-out throughout the process in modelling the grinding wheel surface, could lead to better predictions of grinding force and workpiece surface roughness.

References

Agarwal, S. and Rao, P. (2005) 'A new surface roughness prediction model for ceramic grinding', *Proceedings of the Institution of Mechanical Engineers, Part B: Journal of Engineering Manufacture*, Vol. 219, No. B11, pp.811–821.

Agarwal, S. and Venkateswara Rao, P. (2010) 'Modeling and prediction of surface roughness in ceramic grinding', *International Journal of Machine Tools and Manufacture*, Vol. 50, No. 12, pp.1065–1076.

Agarwal, S. and Venkateswara Rao, P. (2013) 'Predictive modeling of force and power based on a new analytical undeformed chip thickness model in ceramic grinding', *International Journal of Machine Tools and Manufacture*, Vol. 65 pp.68–78.

Bifano, T.G., Dow, T.A. and Scattergood, R.O. (1991) 'Ductile-regime grinding: a new technology for machining brittle materials', *J. Eng. for Industry*, Vol. 113, No. 2, p.184.

Chang, H.C. and Junz Wang, J.J. (2008) 'A stochastic grinding force model considering random grit distribution', *International Journal of Machine Tools and Manufacture*, Vol. 48, Nos. 12–13, pp.1335–1344.

Chen, X. and Rowe, W. (1996) 'Analysis and simulation of the grinding process. Part I: generation of the grinding wheel surface', *International Journal of Machine Tools and Manufacture*, Vol. 36, No. 8, pp.871–882.

Chiang, S.S. (1982) 'The response of solids to elastic/plastic indentation. II. Fracture initiation', *J. Appl. Phys.*, Vol. 53, No. 1, p.312.

Conway, J.C. and Kirchner, H.P. (1980) 'The mechanics of crack initiation and propagation beneath a moving sharp indentor', *J Mater Sci.*, Vol. 15, No. 11, pp.2879–2883.

Kitajima, K., Cai, G.Q., Kurnagai, N., Tanaka, Y. and Zheng, H.W. (1992) 'Study on mechanism of ceramics grinding, CIRP annals', *Manufacturing Technology*, Vol. 41, No. 1, pp.367–371.

Lawn, B.R. and Swain, M.V. (1975) 'Microfracture beneath point indentations in brittle solids', *J. Mater. Sci.*, Vol. 10, No. 1, pp.113–122.

Li, C., Zhang, F., Meng, B., Liu, L. and Rao, X. (2017) 'Material removal mechanism and grinding force modelling of ultrasonic vibration assisted grinding for SiC ceramics', *Ceramics International*, Vol. 43, No. 3, pp.2981–2993.

Malkin, S. and Guo, C. (2008) *Grinding Technology: Theory and Applications of Machining with Abrasives*, 2nd ed., Industrial Press, New York.

Malkin, S. and Hwang, T. (2006) 'Mechanisms for grinding of ceramics', in Marinescu, I. (Ed.): *Handbook of Advanced Ceramics Machining*, CRC Press, New York.

Malkin, S. and Hwang, T.W. (1996) 'Grinding mechanisms for ceramics', *CIRP Annals – Manufacturing Technology*, Vol. 45, No. 2, pp.569–580.

Marshall, D.B., Lawn, B.R. and Evans, A.G. (1982) 'Elastic/plastic indentation damage in ceramics: the lateral crack system', *Journal of the American Ceramic Society*, Vol. 65, No. 11, pp.561–566.

Neo, W.K., Kumar, A.S. and Rahman, M. (2012) 'A review on the current research trends in ductile regime machining', *Int. J. Adv. Manuf. Technol.*, Vol. 63, Nos. 5–8, pp.465–480.

Pinto, F.W., Vargas, G.E. and Wegener, K. (2008) 'Simulation for optimizing grain pattern on engineered grinding tools', *CIRP Annals – Manufacturing Technology*, Vol. 57, No. 1, pp.353–356.

Shaw, M.C. (1972) *Wear of Single Abrasive Grain in Fine Grinding*, Carnegie Press, Pittsburgh, USA.

Stępień, P. (2007) 'Grinding forces in regular surface texture generation', *International Journal of Machine Tools and Manufacture*, Vol. 47, No. 14, pp.2098–2110.

Sun, Y.L., Zuo, D.W., Wang, H.Y., Zhu, Y.W. and Li, J. (2011) 'Mechanism of brittle-ductile transition of a glass-ceramic rigid substrate', *Int. J. Miner Metall Mater.*, Vol. 18, No. 2, pp.229–233.

Tawakoli, T., Kitzig, H. and Lohner, R.D. (2013) 'Experimental investigation of material removal mechanism in grinding of alumina by single grain scratch test', *Advanced Materials Research*, Vol. 797, pp.96–102.

Van Der Zwaag, S., Hagan, J.T. and Field, J.E. (1980) 'Studies of contact damage in polycrystalline zinc sulphide', *J. Mater. Sci.*, Vol. 15, No. 12, pp.2965–2972.

Zahedi, A. (2015) *Improving the Cylindrical Grinding of Engineering Ceramics by Applying Ultrasonic Vibrations and Laser Dressing*, Dissertation, Tehran, Iran.

Zahedi, A. and Azarhoushang, B. (2016) 'FEM based modeling of cylindrical grinding process incorporating wheel topography measurement', *7th HPC 2016 – CIRP Conference on High Performance Cutting*, Vol. 46, pp.201–204.

Zahedi, A., Tawakoli, T. and Akbari, J. (2015) 'Energy aspects and workpiece surface characteristics in ultrasonic-assisted cylindrical grinding of alumina-zirconia ceramics', *International Journal of Machine Tools and Manufacture*, Vol. 90, pp.16–28.